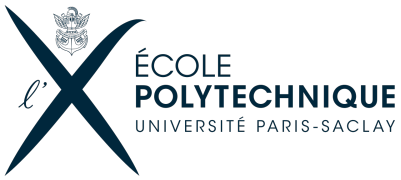

HARVARD
School of Engineering
and Applied Sciences

RESEARCH INTERNSHIP

Mechanics of packed rods

Elodie COUTTENIER

L. MAHADEVAN

H. KING

31 July 2016

Déclaration d'intégrité relative au plagiat

Je soussignée Elodie Couttenier certifie sur l'honneur :

- Que les résultats décrits dans ce rapport sont l'aboutissement de mon travail.

- Que je suis l'auteur de ce rapport.

- Que je n'ai pas utilisé des sources ou résultats tiers sans clairement les citer et les référencer selon les règles bibliographiques préconisées.

Je déclare que ce travail ne peut être suspecté de plagiat.

Signature:

Elodie Couttenier

Le 31/07/2016 à Cambridge

Abstract

Can we create a cohesive object based on many individual particles ? We are interested here in this question which comes originally from the observation of a nest. Made of many different branches, it is indeed solid at the end. We focused our study on a simple model of packing with steel rods and on the diameter-dependant behavior of such a system. This behavior is studied through packing experiments and also compression and tension tests on a pile of these rods.

Résumé

Peut-on créer un objet cohésif à partir d'un ensemble d'éléments individuels ? Nous nous intéressons ici à cette question, provenant de l'observation d'un nid d'oiseau. Construit à partir de nombreuses branches, les nids sont en effet des objets solides. Nous étudions ici un modèle simplifié de compactage de tiges en métal, et nous concentrons particulièrement sur l'effet du diamètre des tiges sur le comportement de ce système. Ce dernier est analysé grâce à des expériences de compactage mais aussi à des tests de compression et traction de ces piles de tiges.

Introduction

Many examples of materials made with ensembles of particles can be found in nature, from sand to birds nests. Most of studies so far concerned spherical particles and their properties as a granular material, like the compaction dynamics [1], the packing fraction or the mechanics of the system.

However materials with a larger aspect ratio are also of great interest. Contrary to spheres, sticks and branches have the ability to create entanglement through mechanical constraints between particles thanks to their flexibility and friction. The coordination number, which is the number of contacts between each rod, is in that case a particularly relevant number which was studied for granular cylinders [2]. Philipse provided a random contact model correlated with experimental datas for the packing of rods [3], as we will discuss later. The effect of the aspect ratio was mainly studied for compaction and coordination number, but the impact of flexibility, which could be responsible for plug formation of granular rods as shown in Blouwolff article, remains unknown.

Other aggregation of particles with different shapes like staples [4] or star-shaped particles [5] were also investigated, especially their stability and collapse.

We will focus here on a simpler shape such as a cylinder with aspect ratio higher than 60. Our goal is to use a model from granular material as simple as piles of rods to approach a system much more complex like a nest. We will start to study the mechanics of these systems mostly through compression and tension experiments.

Methods

We used for our experiments stainless steel cylinders of constant length $L = 50.5$ mm and with varying diameter d from 0.15 to 0.76 mm. This gives us various aspect ratio α between 65 and 330. These rods were cut using at first a laser cutter, then a circular abrasive saw which gave better quality of rods at the edges, and also a lower dispersity in the length ($L = 50.5 \pm 1.6$ mm). The bending stiffness of these wires can be calculated based on $K \sim Er^4$.

The table 1 resumes the main caracteristics of the piles used for the following experiments. The choice of the number of rods N and therefore the total mass M will be discussed in the following part.

Diameter d (mm)	Aspect ratio α	Mass of one rod m_0 (g)	Total mass M (g)	Number of rods N
0.15	333	0.0072	150	21000
0.25	200	0.02	250	12400
0.4	125	0.05	400	7900
0.5	100	0.08	500	6200
0.66	76	0.14	650	4800
0.76	66	0.18	750	4200

Table 1: Properties of the samples

For the study of the packing of rods, we formed samples by dropping rods into a cylinder of diameter $D = 150$ mm, which is 3 times larger than one rod length. Attention was paid to make sure the rods are not entangled before they are dropped. A preliminary study showed the size of the container does not influence properties of the sample unless it is too close to the length of one rod, it leads in that case to a greater effect of the boundaries, as a consequence a significant portion of sticks are vertically aligned.

This container is then attached to a mechanical shaker to excite vertically the sample which allows us to go up to an acceleration of 20 $m.s^{-2}$. Based on the mass of the pile and its size, we can extract the number of rods as well as the packing fraction ϕ which is given by the following equation :

$$\phi = \frac{Volume\ of\ the\ rods}{Total\ volume\ occupied\ in\ the\ cylinder} = \frac{N\pi(\frac{d}{2})^2 L}{\pi(\frac{D}{2})^2 h}$$

The height h is determined thanks to images taken regularly during the packing. Particular attention was paid to take images when the rods are not moving. To that end, a microcontroller was used to synchronize the motor and the camera. Given the fact that the density of rods is higher at the bottom than at the top of the cylinder, we had to set a threshold for the determination of the pile's height. An example is given on the figure 1, by removing the few rods at the top, we can reach a more reliable volume fraction.

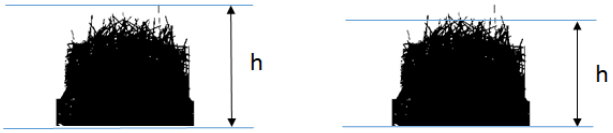

(a) (b)

Figure 1: Images of a pile of rods (a) Height without any threshold which takes into account every single rod. (b) Height with a given threshold

With this process, we could see the volume fraction increasing with the number of excitations and reaching a steady state where this final volume fraction ϕ_f was close to the one predicted in the article [3]. Indeed, they predicted that

$$\phi_f\ \alpha \simeq constant \tag{0.1}$$

with $\alpha = \frac{L}{d}$ the aspect ratio. We encountered few problems with this set-up among which the characterization of the movement that was unclear depending on the speed. Indeed, increasing the frequency of the excitation makes the packing more efficient but in that case, the acceleration goes to a value higher than g and the rods don't touch the support anymore when it is going down. The movement is then non-continuous leading to a collision between the rods and the plateform. The control of the motor speed was also not well charaterized.

After few experiments, we determined that the way of packing was not so determinant in the mechanical properties of the pile. A new protocol was then chosen, the rods were poured in the container, a disc of cardboard was dropped on the top of the packing and the container was turned upside down several times. This allows to get a sample with a top side rather flat, compared to the first set-up.

For the purpose of these experiments, we had to choose a constant parameter for each diameter of rods. At first, a same number of rods $N \simeq 6000$ was used for each of them but given the difference in volume fraction, the heights of the piles were completely different, this height reaches only 70 mm for the thinner rods which is barely more than a rod length. Consequently, the height was kept always at the same value around $h \simeq 110$ mm and since $\phi\alpha$ is a constant as seen previously, this defines the number of rods we have to put in the system. Figure 2 shows the volume fraction used for the following experiments, the constant $\phi\alpha$ is equal to 3.2 in our case, compared to the value 5.4 found in the litterature for the maximum packing fraction. Variation in the height can occur during the packing process, the error bars here correspond to $\Delta h = \pm 10$ mm.

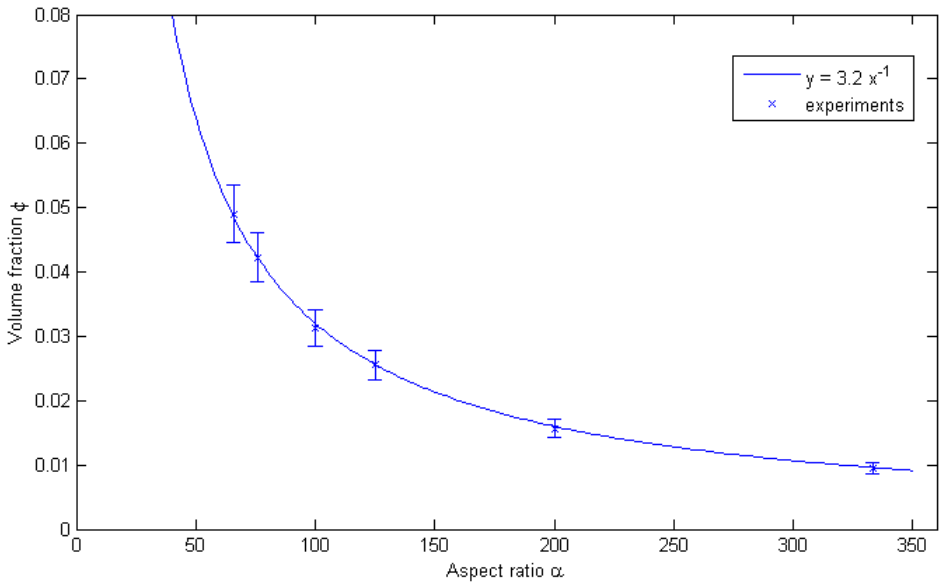

Figure 2: Volume fraction as a function of the aspect ratio.

An electromechanical testing machine was used to realize both compression and tension tests on our samples, as shown on figure 3. The diameter of the cylinder was then D = 153 mm so we can apply a compression force while keeping a confined system. The load and the displacement can be measured. For the tension experiments, the rods are dropped in a layer of few millimeters of an epoxy resin in a dish, the sample is returned to attach the top of the pile the same way. One endcap is attached to the load cell and is pulled, while the other one is fixed.

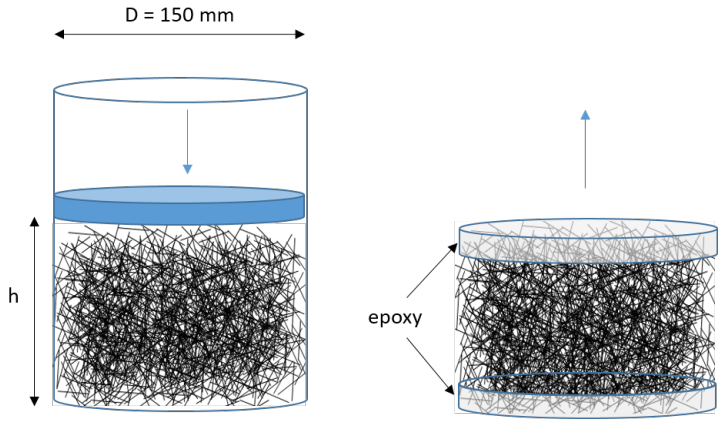

Figure 3: Rods are dropped into a cylinder of diameter $D = 150$ mm. They are then put under a compression test without removing the container (left) or a tension test by fixing both rods at the top and bottom with epoxy (right).

Results & discussion

1 Compression

A typical curve of stress-strain for our samples is shown on figure 4. Cycles are done by pushing on the piles of sticks up to a given strain and then coming back to the initial height. We can see on these curves the presence of hysteresis, which is characteristic of the plasticity in this system. Indeed, by applying a stress on the rods, we are doing both elastic and plastic deformation. The first one is linked to the fact that rods are bending under an applied force, while the second is due to their movement, they can slide or rotate against each other.

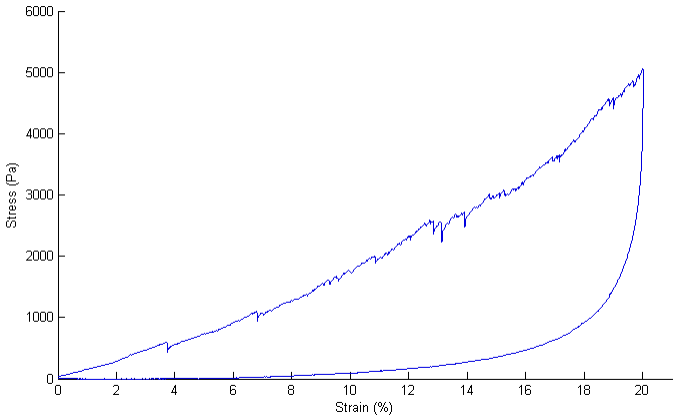

Figure 4: Stress-strain curve for a pile of rods of diameter 0.5 mm with an initial height of 113 mm. The load is increasing as the sample is compressed up to 20% of strain, then the load is removed. The speed is 10 mm/min.

This experiment was done for the different rods diameters presented previously, and figure 5 shows the stress at 10% and 20% of strain for each sample as a function of the diameter. The error bars come from the difficulty of reproducing exactly the same experiment each time, and are based on 4 different tests.

We can fit theses curves with a power law, the stress goes with $d^{2.5}$. The stiffer an individual rod is, the stiffer the packing will be under compression. We could have expected it to be proportionnal to d^4 because this power is linked to the bending stiffness. We can explain the difference by the fact that

the number density is not the same for these various sticks. As explained before, the volume fraction is significantly different from one kind of rod to another. Rather then considering the volume fraction which takes the volume of one rod into account, we can look at the number density $n = \frac{N}{\pi(\frac{D}{2})^2 h}$ which is the number of rods per unit volume. For a sample of a given rods diameter, increasing the number of rods N for a same volume would make it stiffer. This means the load at a given strain would increase with the number density n. We were able to notice this effect, but unfortunately, not to reach significant various density for a particular sample to verify properly this hypothesis. But in our case, $\phi\alpha = cst$ is equivalent to say that $nd = cst$, this could explain why the power is less than 4.

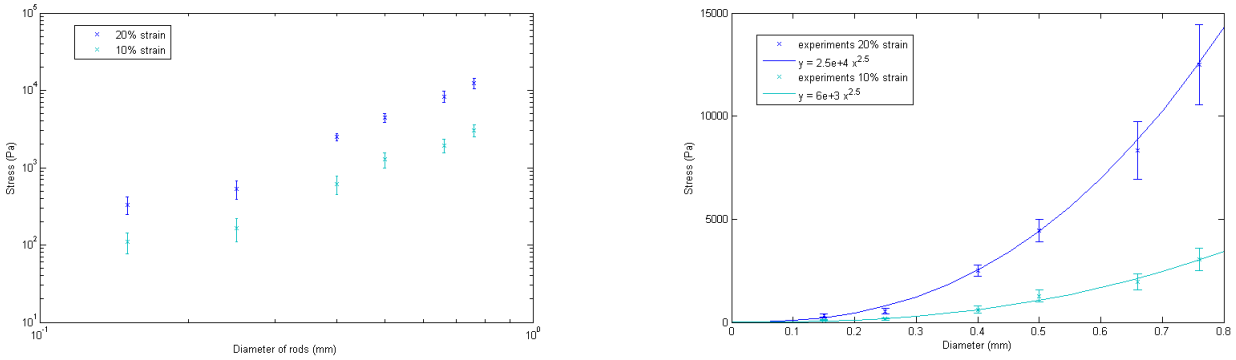

Figure 5: Stress at a given strain, here for 10% and 20% of strain for various diameters of rods. The figure is shown in a log-log scale on the left and was fitted with $d^{2.5}$ on the right.

2 Elasticity

We have seen previously that the plasticity plays an important role in our system and is responsible for the hysteresis we see on the curves, which means that energy has been dissipated or stored in the sample. Looking at much smaller deformation could be a way to reach at some point a pure elastic deformation. Figure 6 shows an example of cycles done around 0% of strain, in compression (positive strain) and tension (negative strain). The strain was increased from 0.5% to 4%. The hysteresis is still observed whatever the deformation.

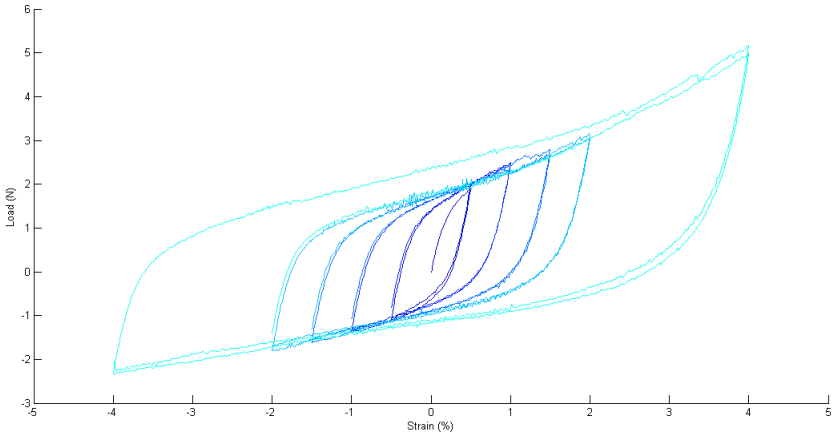

Figure 6: Cycles both in compression (positive strain) and tension (negative strain) for a sample made with rods of diameter 0.25 mm. Consecutive cycles were done increasing each time the strain ($\pm 0.5\%$ to $\pm 4\%$).

The strain rate was also changed to see if this phenomena could be due to dissipation. In that case, slowing down the strain rate would reduce the hysteresis. A factor of 50 in the speed doesn't seem to have any effect on the curve (figure 7), this means our system of N rods always presents some plasticity and we can't extract a real Young modulus as we could expect for a classic material.

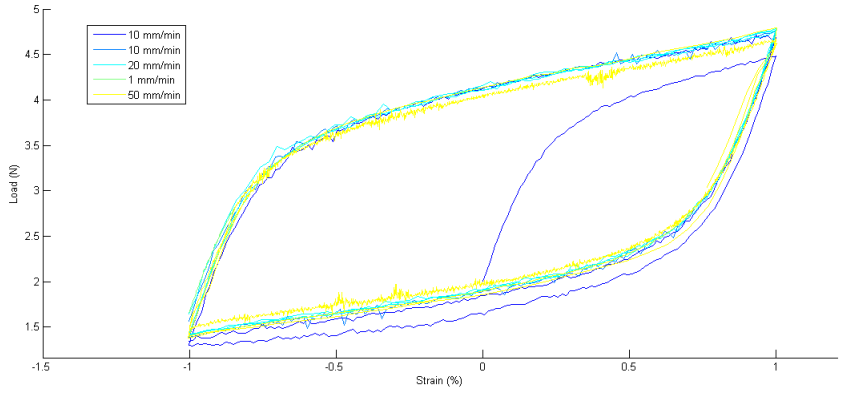

Figure 7: Cycles between -1% and 1% strain for the sample with rods of diameter 0.25 mm with different strain rates, between 1 mm/min to 50 mm/min. The shape of the curve doesn't change with the speed.

3 Stress softening and Mullins effect

Mullins effect ?

We are now interested in the memory of our system. To study that, cycles with increasing strain were done as we can see on figure 8(a). The system is compressed up to 3% strain, then we are unloading it (the load is coming back to the initial point, the 0% strain of the initial state is taken as a reference), and the sample is compressed again but to a higher deformation this time (3% more each time, keeping the initial height as a reference). We observed a stress softening for deformation lower or equal to the maximum ever applied. But once this point is reached and the displacement is still increasing, the load is going back to the same path as it would be if it was a simple compression without cycling, which is represented by the red curve on this figure.

This phenomenon is interesting because it means that we are progressively damaging the sample while increasing the compression : a new part of the system is involved in a plastic deformation each time it experiences a bigger strain. We can compare this effect with the one commonly known as the Mullins effect, which is usually present in rubber and generally associated with bond rupture, disentanglement or molecules slipping. Indeed, as shown in figure 8(b) taken from [6], the same behavior is observed in elastomers where we can see the importance of the maximum load previously encountered.

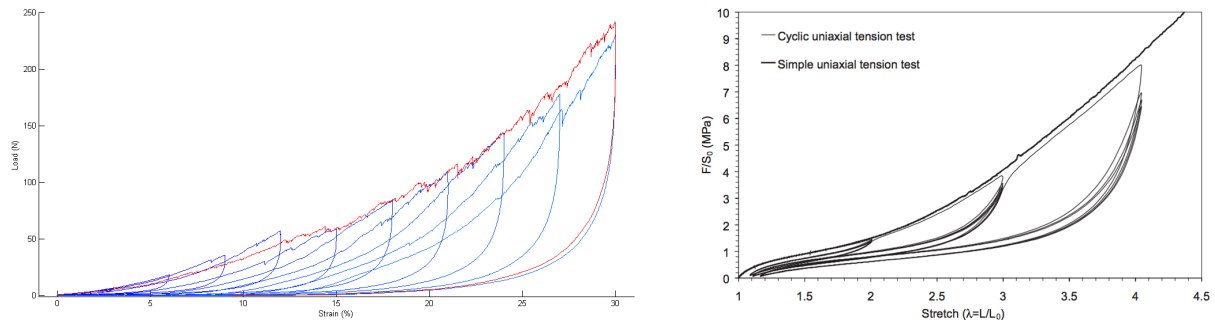

(a) (b)

Figure 8: Cyclic compression with increasing strain and simple compression for a pile of rods defined previously (a) and an elastomer (b) taken from [6].

Aging over many cycles

Instead of increasing the deformation each time, we can look closer at the stress softening by doing the same cycle to the same extension many times. It was done on the figure 9(a) and in that case, the load at a given displacement is decreasing with the number of cycles. The main decrease occures between the first and the second cycle, then it keeps decreasing slowly. And this behavior is also noticed in elastomers, as shown in 9(b) taken from [8]. We observe here the same hysteresis and stress softening at a given displacement.

This load decreasing as a function of the number of cycles is shown below on figure 10(a) in a semi-logarithmic scale and for several rods diameters. It is still not clear if this is a logarithmic decrease, as it was claimed in the article [7] with the figure 10(b) for filled rubber. Indeed many relaxations and aging happen to be logarithmic, as it is described in [9] for crumpled sheets for example.

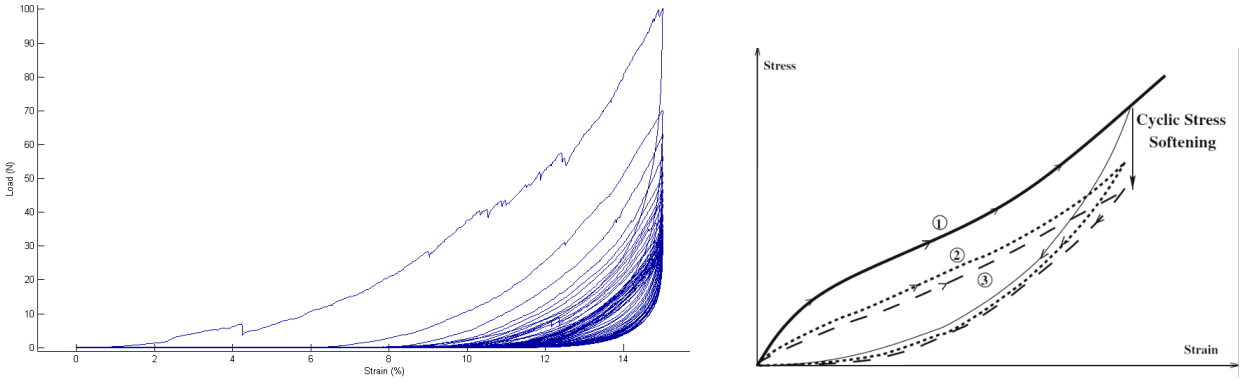

(a) (b)

Figure 9: (a) Load as a function of the displacement for many cycles to a given extension (here 15% of the initial height). (b) Stress-strain curve for a classic rubber where we can see the stress softening, from [8].

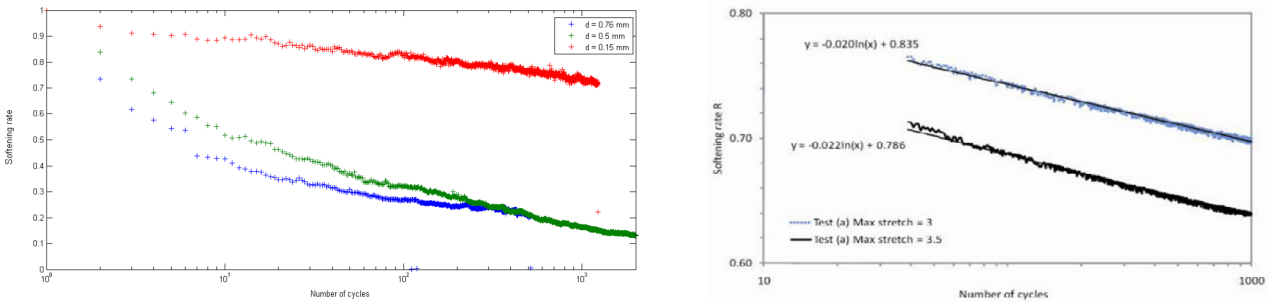

(a) (b)

Figure 10: Softening rate, which is the load at the maximal extension for each cycle over the load for the first cycle, as a function of the number of cycles (a) for 3 various rods diameters. (b) for filled rubber, from [7]

.

4 Tension test

Based on our observations, we could claim that the behaviors in compression and tension of our samples would not depend in the same way of the diameter. Experiments of tension were then realized with the protocol explained previously. Images of these experiments were taken and shown on the figure 11 below. From these, we can clearly see the difference in cohesion between the samples. The thinner rods (a) seem to be more difficult to pull apart than the bigger rods (b) whose sample is breaking quickly.

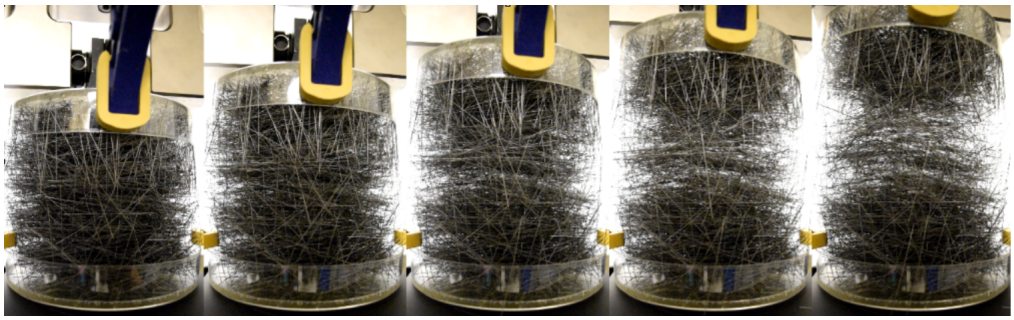

(a)

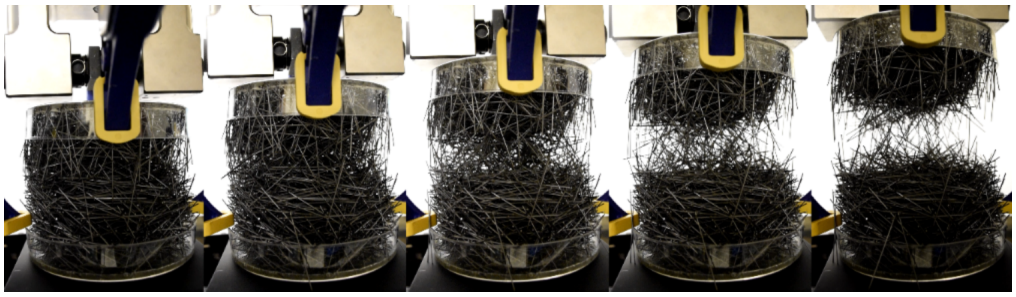

(b)

Figure 11: Successive images during a tension test for 2 different piles of rods. (a) d = 0.25 mm and the top layer was moved 18 mm between each image. (b) d = 0.76 mm and the top layer was moved of 10 mm.

To further investigate this cohesion and entanglement which seems to be higher in case of small diameter, we now look at the stress-strain curve. One typical example is represented on figure 12, where the load and the strain are negative due to the fact the sample is now in tension instead of compression.

The curve has to be read from right to left, at first the load is increasing (in negative value), then it is decreasing while the rods are separated. At the end, the sample is broken and there is still a non zero load because of the remaining part of the sample which is maintained at the top, as we can see on the previous images.

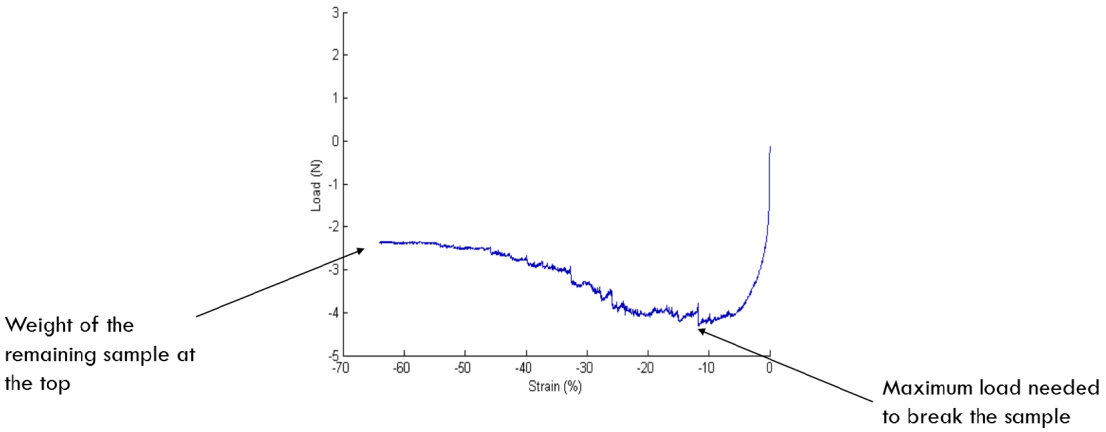

Figure 12: Load as a function of the strain for one sample in tension. The curve should be read from right to left while the sample is being pulled.

We also have to notice that this load is taking two effects into account. The first one is linked to the weight of the rods lifted (it is harder to pull on the rods with a large diameter because the total weight of the sample is larger) and it is also an indicator of the entanglement, or in other words how hard it is to break the sample. These two effects being linked in opposite way with the diameter of the rods, it is necessary to remove the part associated with the weight. To do so, a scale was used to follow the weight of the sample at the same time. This gives us for instance the figure 13. Based on these two curves (one deduced from the weight read on the scale, and the other one obtained with the mechanical tester), we can think of the area inbetween as the energy provided to break the sample and disentangle the rods.

Let's look at this area as a relevant parameter to characterize the cohesion of our system. The displacement at complete break can also be used. The figure 14 shows both parameters as a function of the rods diameter. The trend is clearly a decrease with a bigger diameter.

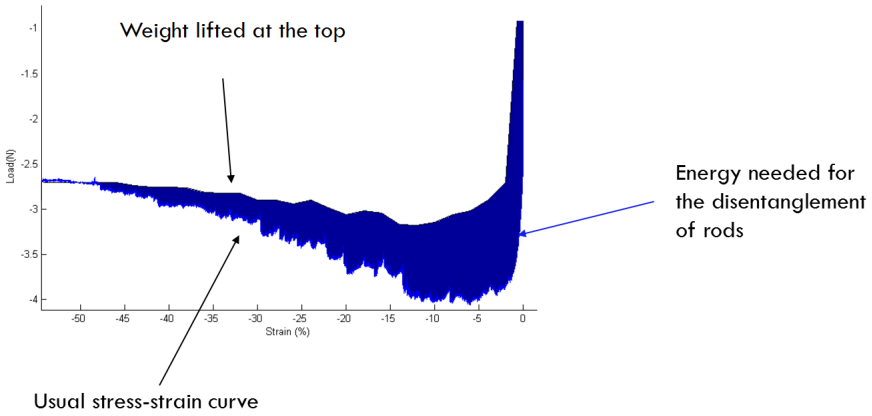

Figure 13: Load (N) as a function of the strain (%) for one sample in tension. The bottom curve corresponds to the usual curve given by the tester and the top curve is the weight held at the top.

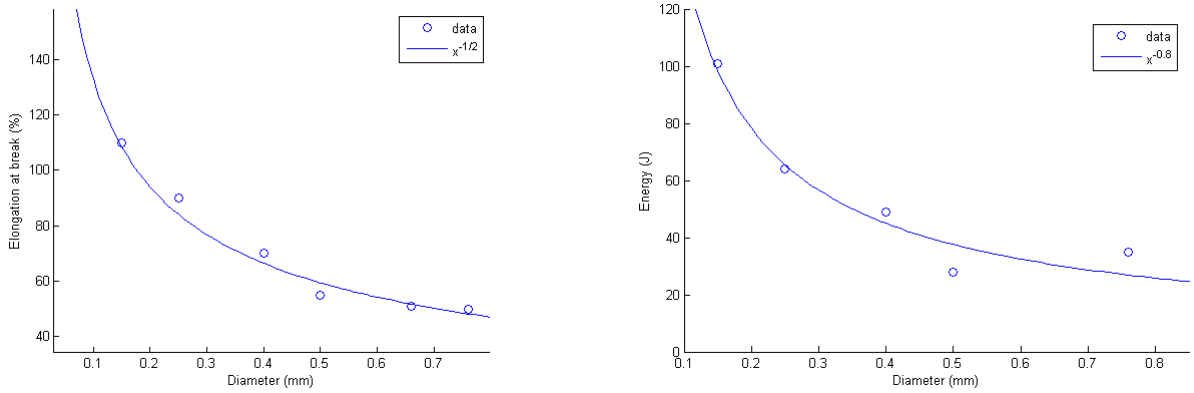

Figure 14: Elongation at break (%) and energy needed to break the sample (J) as a function of the rods diameter (mm).

.

Conclusion

We have presented here the first datas obtained on this subject. As explained at the beginning, the mechanics of systems such as this aggregate of elongated particles was not studied yet. Here is a first attempt to characterize this system, in this purpose, packing, compression and tension experiments were done. This was mainly an exploratory work, and many questions were asked concerning the response of the system to a mechanical stress, the presence of elasticty or plasticity, or the aging. We were able to show some partial answers, even if there is no model yet behind these results. We can mention the diameter dependence of the response in compression or tension which is one of the main results we would like to explain. The cohesion created by assembling thin rods is also a point of interest which can be linked to the idea of entanglement in birds nest. We have also noticed an interesting phenomenon with the stress softening that can be compared with the one occuring in elastomers.

We also need to mention another approach we started to study is an X-ray computed tomography. We used this technology to scan several samples with or without load and for different rods diameters. A scan allows us to have a 3D reconstruction of the rods, and with an advanced image analysis, we should be able to identify each rod and determine the number of contacts called the coordination number as we mentionned at the beginning. Another hope is to be able to get the distribution of the stress from the curvature of the rods and also look at the propagation of this stress when a load is applied. Connecting these results with the macroscopic information from compression and tension test would be of great interest.

References

[1] Philippe, P. and Bideau, D., 2002. Compaction dynamics of a granular medium under vertical tapping. *EPL (Europhysics Letters)*, 60(5), p.677.

[2] Blouwolff, J. and Fraden, S., 2006. The coordination number of granular cylinders. *EPL (Europhysics Letters)*, 76(6), p.1095.

[3] Philipse, A.P., 1996. The random contact equation and its implications for (colloidal) rods in packings, suspensions, and anisotropic powders. *Langmuir*, 12(5), pp.1127-1133.

[4] Gravish, N., Franklin, S.V., Hu, D.L. and Goldman, D.I., 2012. Entangled granular media. *Physical review letters*, 108(20), p.208001.

[5] Zhao, Y., Liu, K., Zheng, M., Barés, J., Dierichs, K., Menges, A. and Behringer, R.P., 2016. Packings of 3D stars: stability and structure. *Granular Matter*, 18(2), pp.1-8.

[6] Julie Diani, Bruno Fayolle, Pierre Gilormini, 2009. *European Polymer Journal*, pp.601-612.

[7] M. Brieu, J. Diani, C. Mignot, C. Moriceau, 2010. *Procedia Engineering 2*, 1291–1296

[8] S. Cantournet, R. Desmorat, J. Besson, 2009. *International Journal of Solids and Structures*, 2255–2264

[9] Amir, A., Oreg, Y., Imry, Y., 2012. On relaxations and aging of various glasses. *Proceedings of the National Academy of Sciences*, 109(6), 1850-1855.